Supporting Information

for

Monolayer Nitrides Doped with Transition Metals as Efficient Catalysts for Water Oxidation: the Singular Role of Nickel

Qiuhua Liang[1], Geert Brocks[2,3,4], Xueqing Zhang[1,2], Anja Bieberle-Hütter[1,2]*

1 Electrochemical Materials and Interfaces (EMI), Dutch Institute for Fundamental Energy Research (DIFFER), De Zaale 20, 5612 AJ, Eindhoven, the Netherlands

2. Center for Computational Energy Research (CCER), P.O. Box 513, 5600 MB, Eindhoven, the Netherlands

3. Department of Applied Physics, Eindhoven University of Technology, P.O. Box 513, 5600MB, Eindhoven, the Netherlands

4. Computational Materials Science, Faculty of Science and Technology and MESA+ Institute for Nanotechnology, University of Twente, P.O. Box 217, 7500 AE Enschede, the Netherlands

*A.Bieberle@differ.nl

Zero-point energy and entropic correction

Zero-point energies (ZPE) and entropic corrections (*TS*) at $T = 300$ K are listed in Table S1 for the molecules in the gas phase (H_2O, H_2 and O_2), and for the adsorbed species (*OH, *O and *OOH). The values for the H_2O, H_2 and O_2 molecules in the gas phase are taken from Ref. 1. The ZPE and *TS* values of the adsorbed species are determined from the vibrational frequencies as discussed in the main text. The same values are used for all systems, as the vibrational frequencies are not very dependent on the substrate.

Table S1. Zero-point energies (ZPE) and entropic corrections (*TS*) at T = 300 K for the molecules in the gas phase (H_2O, H_2 and O_2) and for the adsorbed species (*OH, *O and *OOH). The same values are used for all systems. The values for the molecules in the gas phase are taken from Ref. 1.

Species	ZPE (eV)	*TS* (eV)
H_2O	0.56 [1]	0.67 [1]
H_2	0.27 [1]	0.41 [1]
O_2	0.10 [1]	0.64 [1]
OH*	0.34	0.06
O*	0.06	0.01
OOH*	0.43	0.07

Optimized structures of TM-doped AlN and GaN with/without adsorbants

Figure S1 shows the optimized structures of (TM-doped) AlN and GaN monolayers in top and side views, without and with adsorbants. Figure S1a shows the pristine AlN and GaN cases, and Figures S1 b-k illustrate the TM-doped AlN and GaN systems.
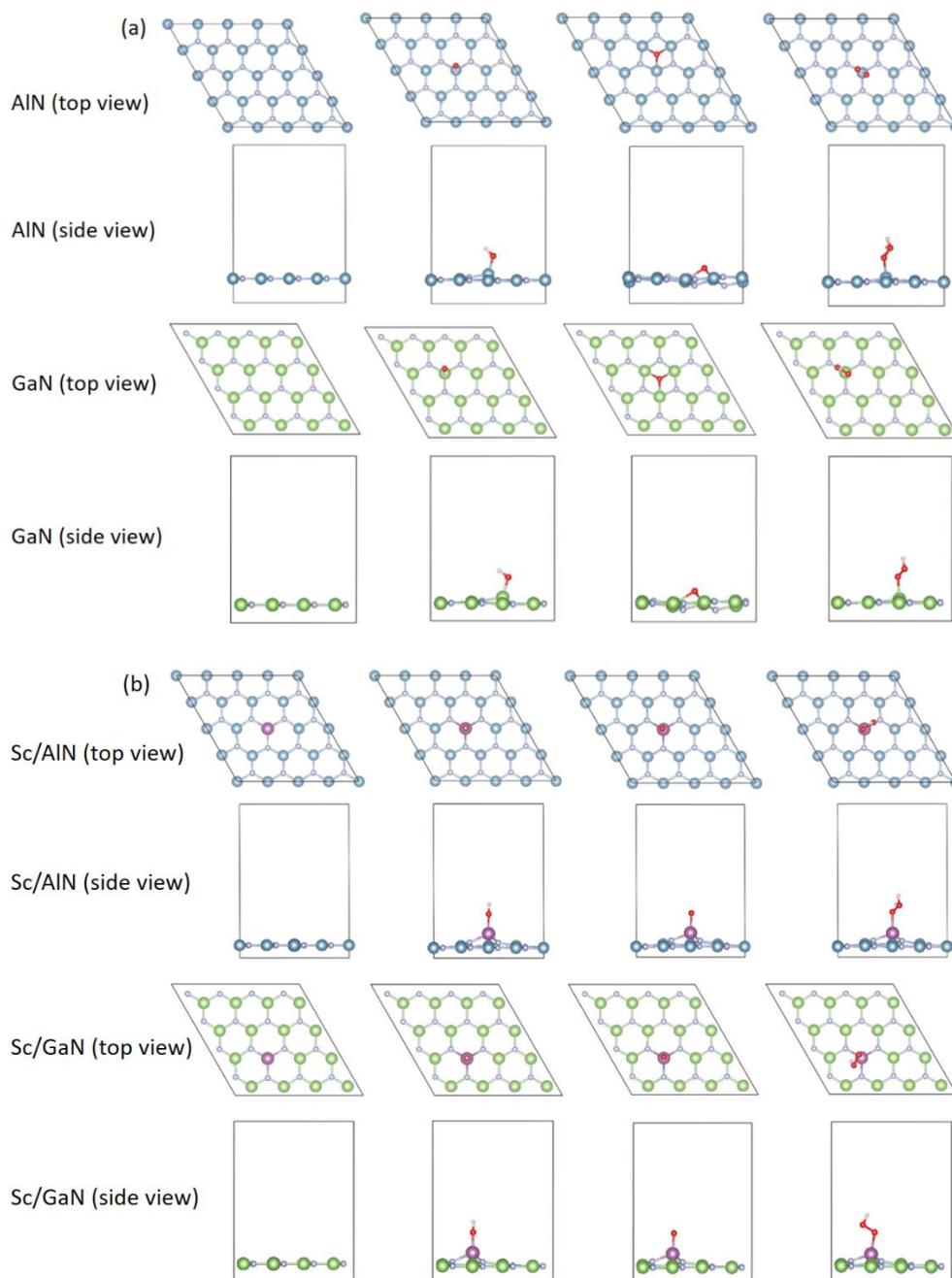
(c)
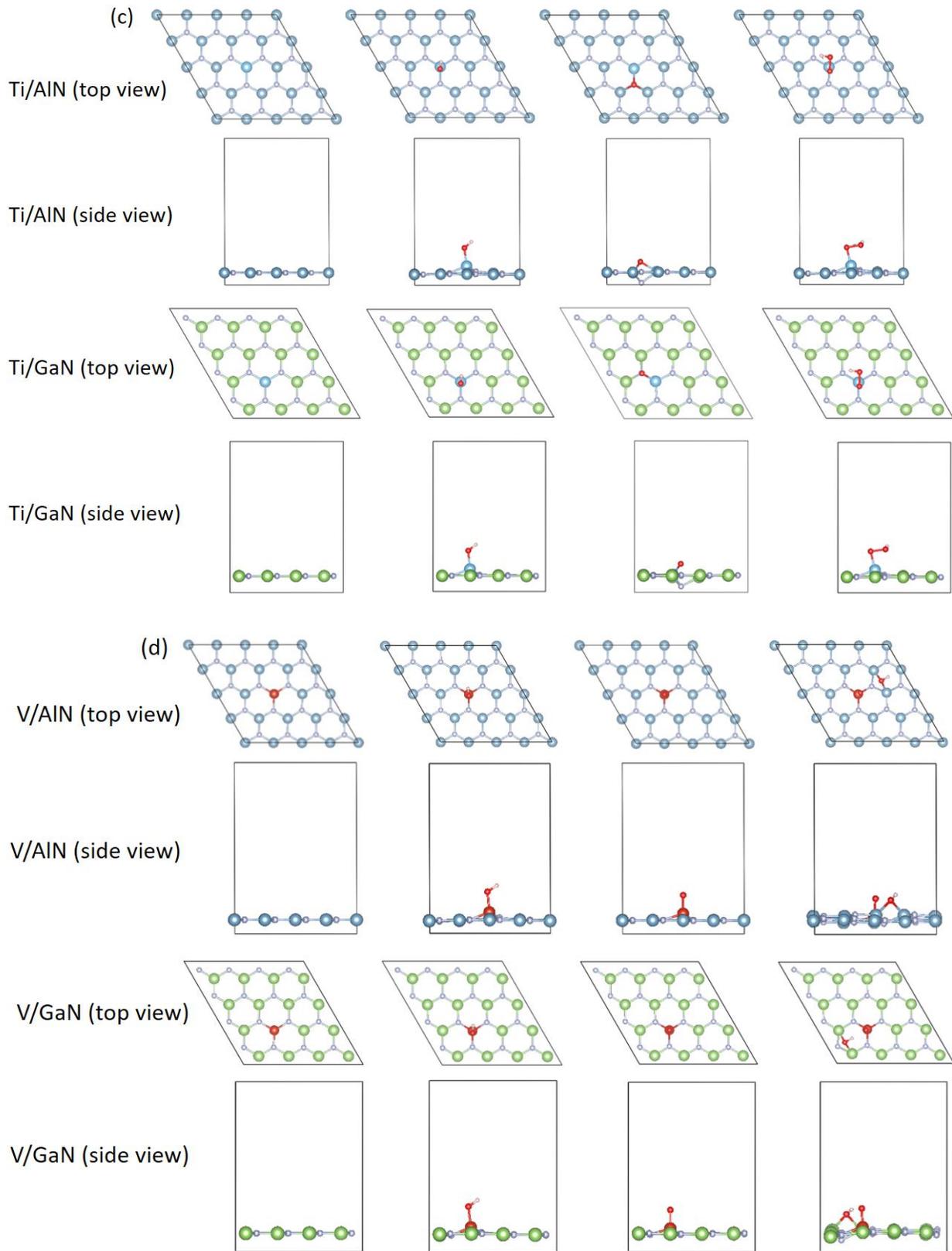
Ti/AlN (top view)

Ti/AlN (side view)

Ti/GaN (top view)

Ti/GaN (side view)

(d)

V/AlN (top view)

V/AlN (side view)

V/GaN (top view)

V/GaN (side view)

Continue on next page

(e)

Cr/AlN (top view)

Cr/AlN (side view)

Cr/GaN (top view)

Cr/GaN (side view)

(f)

Mn/AlN (top view)

Mn/AlN (side view)

Mn/GaN (top view)

Mn/GaN (side view)

Continue on next page

(g)

Fe/AlN (top view)

Fe/AlN (side view)

Fe/GaN (top view)

Fe/GaN (side view)

(h)

Co/AlN (top view)

Co/AlN (side view)

Co/GaN (top view)

Co/GaN (side view)

(i)

Ni/AlN (top view)

Ni/AlN (side view)

Ni/GaN (top view)

Ni/GaN (side view)

(j)

Cu/AlN (top view)

Cu/AlN (side view)

Cu/GaN (top view)

Cu/GaN (side view)
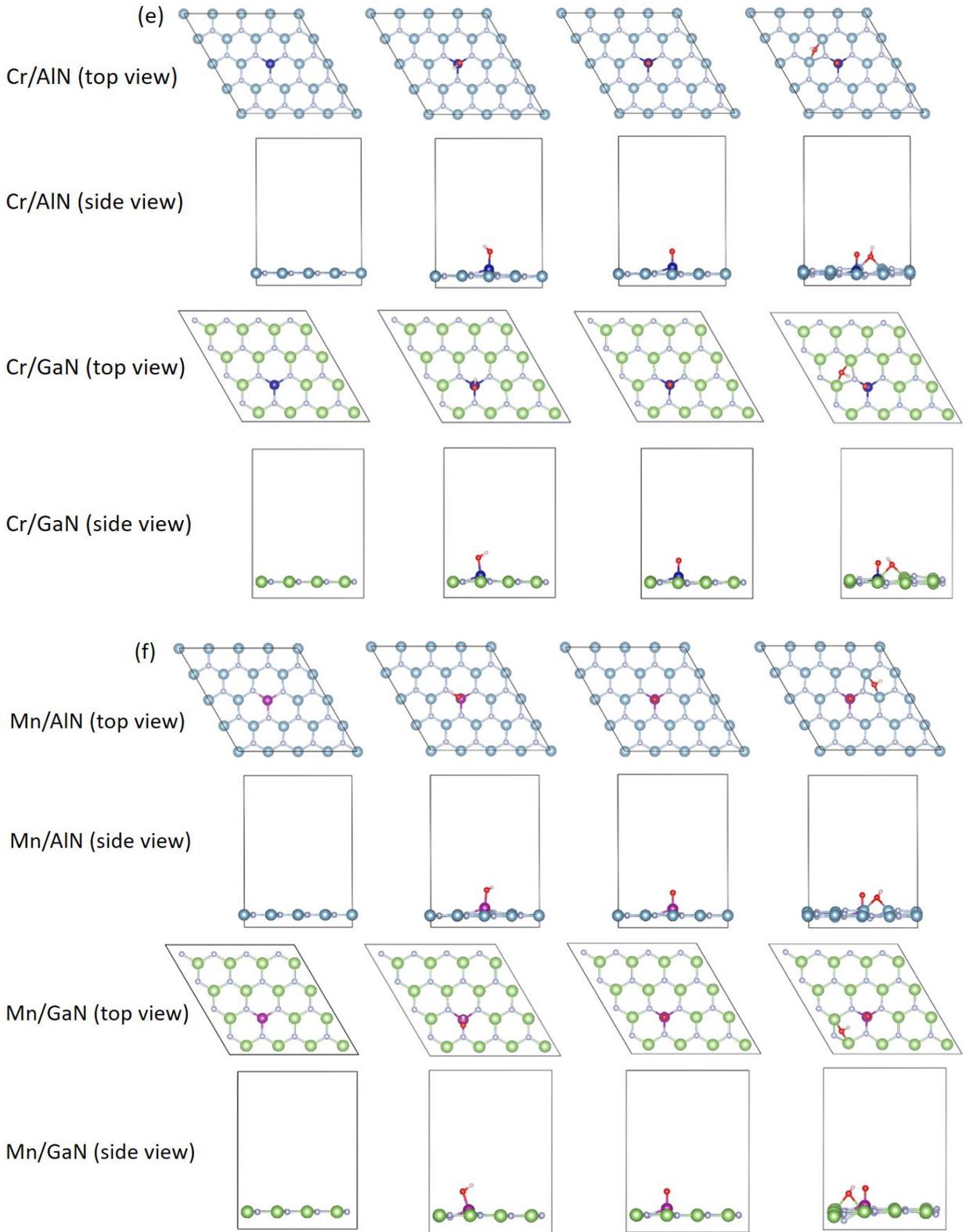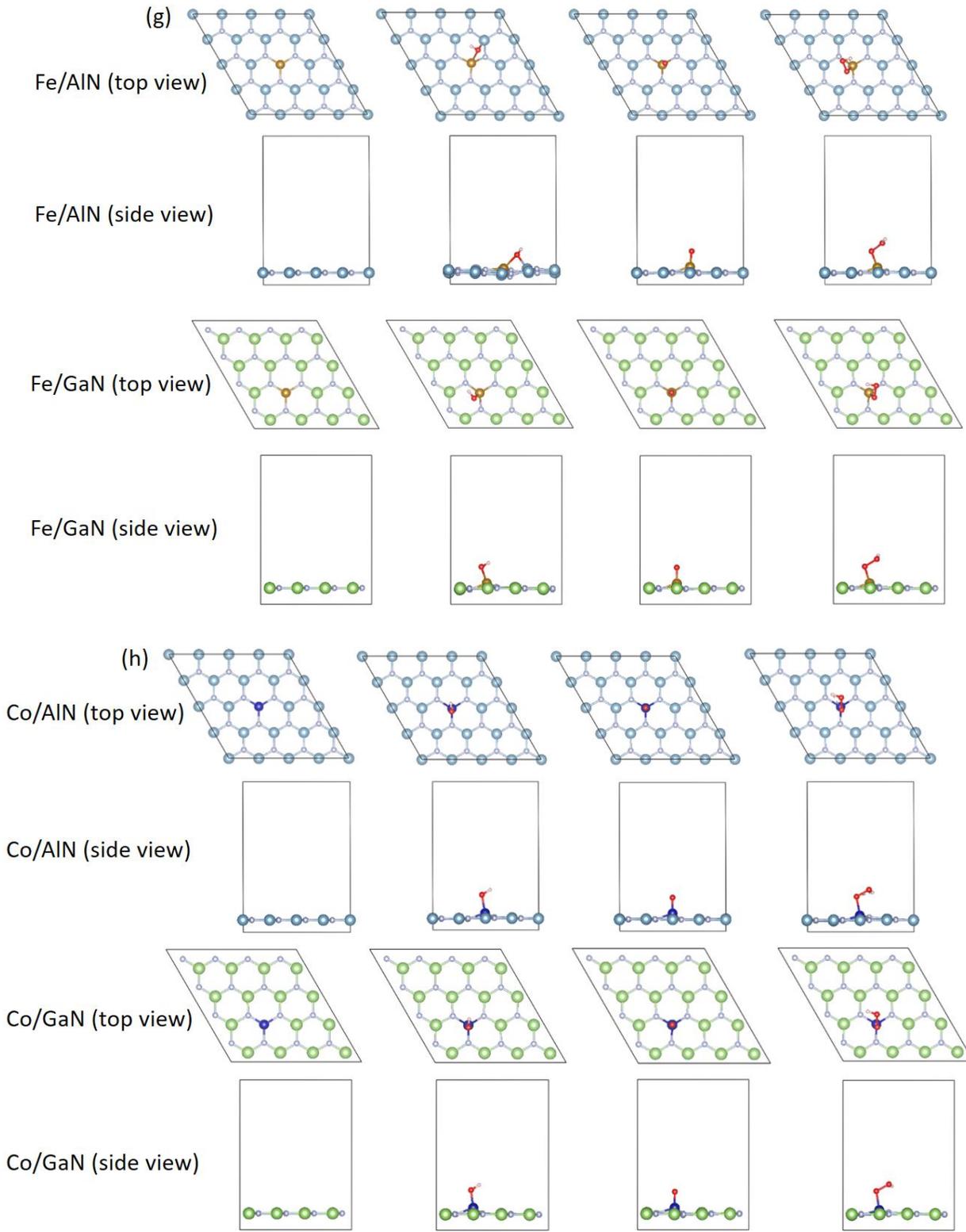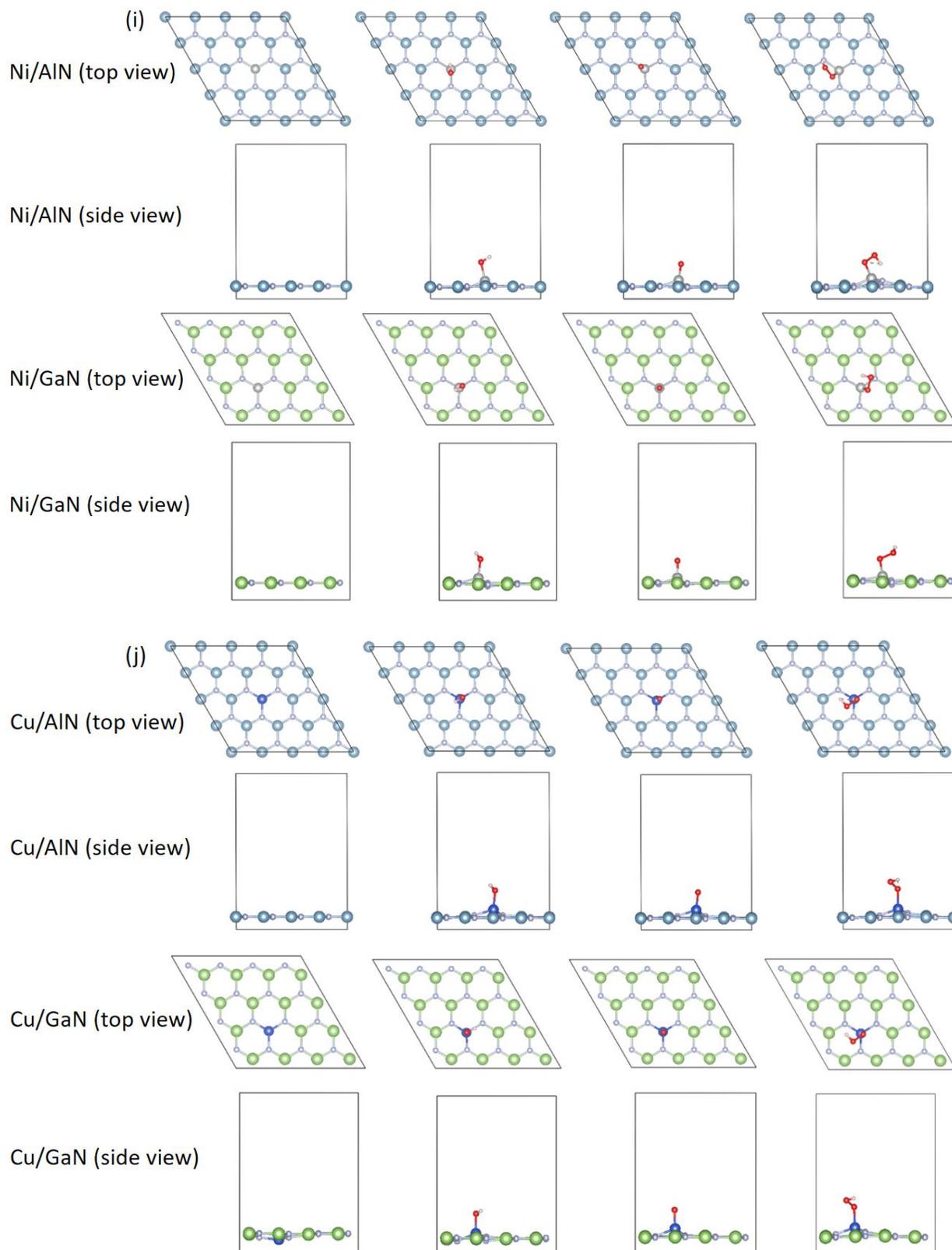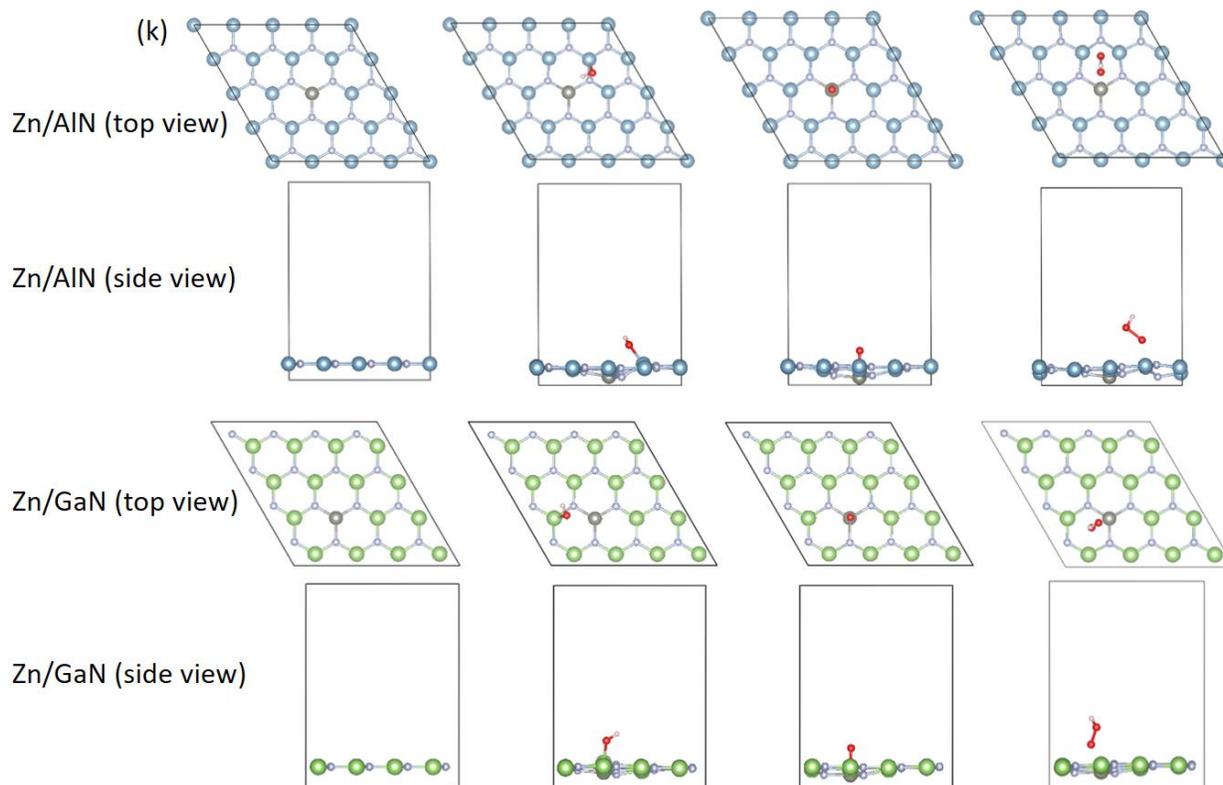
Figure S1. Optimized structures of (TM-doped) AlN and GaN monolayers in top and side views, without and with adsorbants; (a) pristine AlN and GaN; (b) Sc-doped_AlN and Sc_GaN; (c) Ti_AlN and Ti_GaN; (d) V_AlN and V_GaN; (e) Cr_AlN and Cr_GaN; (f) Mn_AlN and Mn_GaN; (g) Fe_AlN and Fe_GaN; (h) Co_AlN and Co_GaN; (i) Ni_AlN and Ni_GaN; (j) Cu_AlN and Cu_GaN; (k) Zn_AlN and Zn_GaN. The colored spheres represent, blue: Al, silver: N, red: O, white: H, green: Ga.

Gibbs free energies

Table S2 lists the Gibbs free energies calculated for the electrochemical reaction steps (4)-(7) in the main text according to Eqs. (10)-(13), for pristine and TM-doped AlN and GaN. As the Zn dopant is totally inert, we omit it from the Table. As some intermediates do not adsorb (meta)stably on some dopants, those Gibbs free energies could not be calculated; we mark these cases with "/".

Table S2. Gibbs free energies (eV) calculated for the elementary reaction steps (4)-(7) in the main text according to Eqs. (10)-(13), for pristine and TM-doped AlN and GaN. / means that the intermediates do not adsorb stably or metastably on the dopants. The overpotential-determining reaction steps are marked in red.

	AlN	Sc	Ti	V	Cr	Mn	Fe	Co	Ni	Cu
ΔG_1	1.54	0.64	-1.63	-1.06	-0.53	0.13	0.18	1.34	1.61	1.89
ΔG_2	1.97	2.50	1.60	-0.55	0.28	0.07	1.45	0.80	1.22	2.01
ΔG_3	1.18	0.73	1.68	/	/	/	2.18	2.30	1.46	0.95
ΔG_4	0.23	1.05	3.27	/	/	/	1.11	0.48	0.63	0.07
	GaN	Sc	Ti	V	Cr	Mn	Fe	Co	Ni	Cu
ΔG_1	1.78	0.71	-1.53	-1.05	-0.60	0.21	0.71	1.34	1.53	2.03
ΔG_2	1.96	2.51	2.09	-0.35	0.32	0.09	1.04	0.85	1.29	1.87
ΔG_3	1.06	0.73	1.17	/	/	/	2.13	2.21	1.60	1.05
ΔG_4	0.12	0.97	3.19	/	/	/	1.04	0.52	0.50	-0.03

Spin-polarized projected density of states (PDOS) of TM-doped AlN and GaN

Figures S2 and S3 show the spin-polarized projected density of states (PDOS) of all TM doped AlN and GaN monolayers. In the case of AlN, only the *p*-orbital contribution is shown (Al has no electrons in a *d* orbital); for GaN, both *p*- and *d*-orbital contributions are plotted. Positive values indicate the PDOS for spin-up electrons, and negative values indicate –PDOS for spin-down electrons. The Fermi energy is put at zero energy, as indicated by the vertical dotted line.
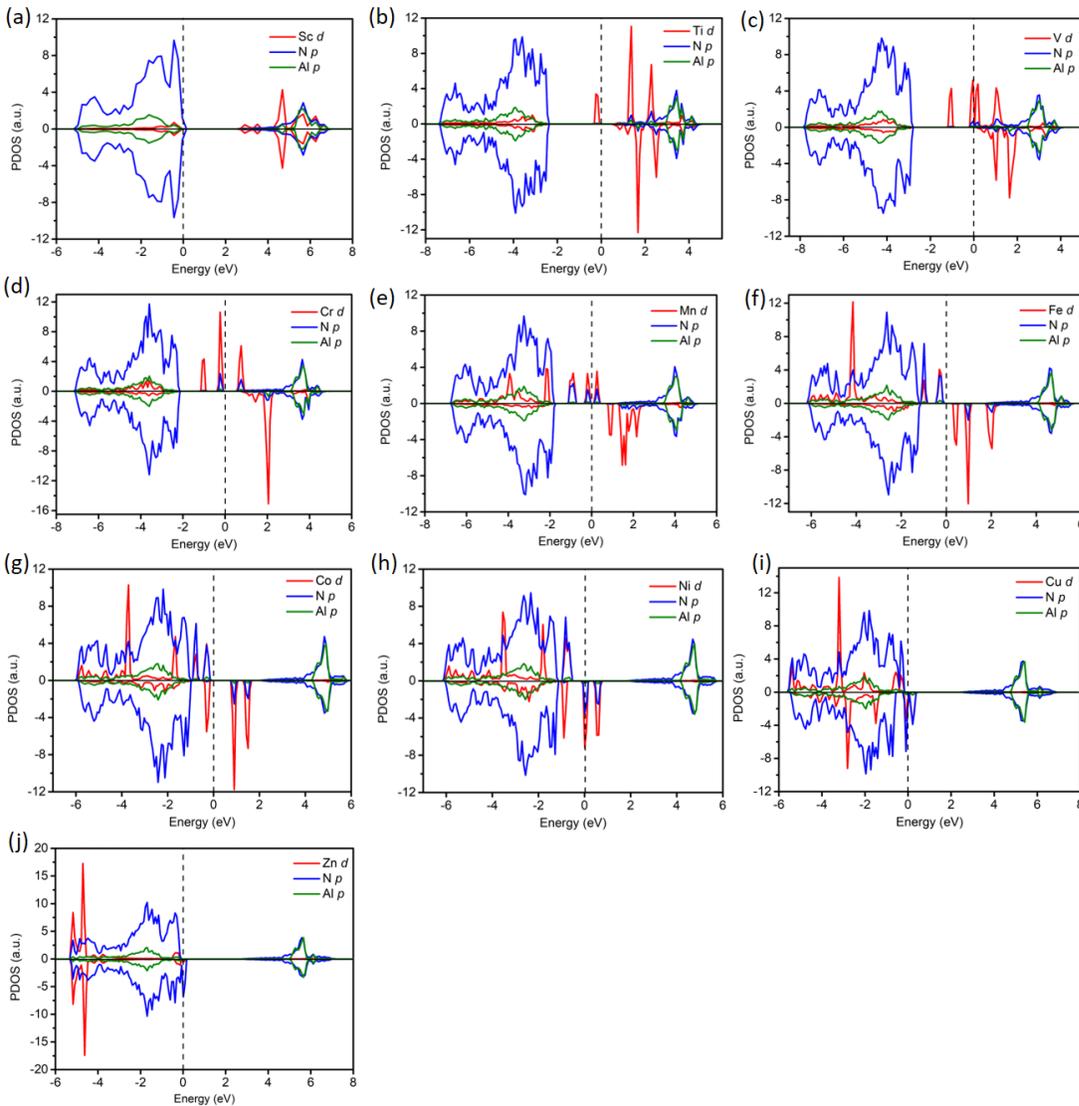
Figure S2. PDOS of TM-doped AlN with the TM atoms (a) Sc, (b) Ti, (c) V, (d) Cr, (e) Mn, (f) Fe, (g) Co, (h) Ni, (i) Cu and (j) Zn.
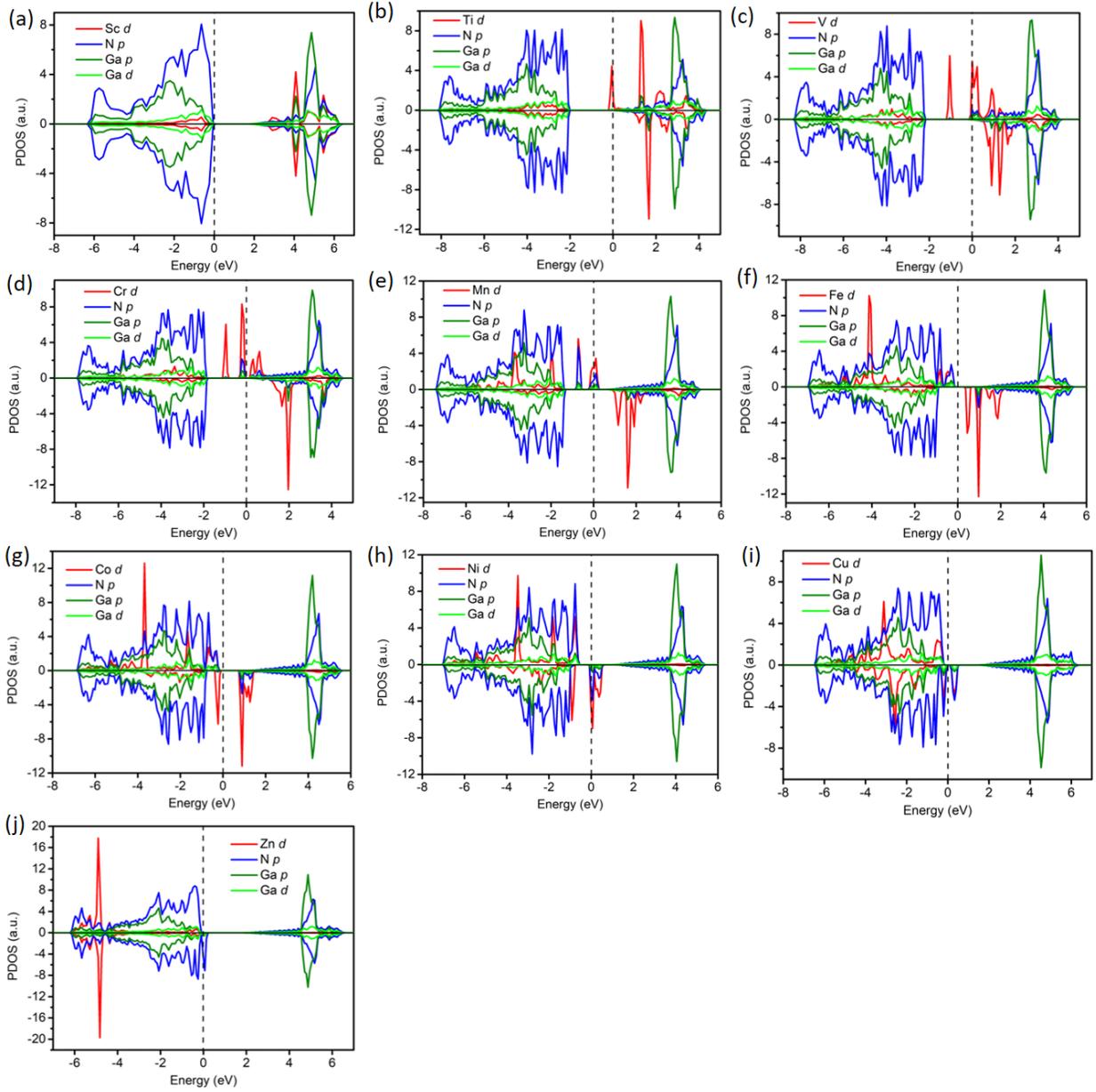
Figure S3. PDOS of TM-doped GaN with the TM atoms (a) Sc, (b) Ti, (c) V, (d) Cr, (e) Mn, (f) Fe, (g) Co, (h) Ni, (i) Cu and (j) Zn.

Figure S4 and S5 show the PDOS of TM ions in TM-doped AlN and GaN monolayers, resolved into contributions of the individual d orbitals. In trigonal planar symmetry environment, the five

degenerate $3d$ orbitals are split into one a singly degenerate state d_{z^2}, and two doubly degenerate states d_{xz}, d_{yz}, and $d_{x^2-y^2}, d_{xy}$, with the energy ordering $d_{z^2} < d_{xz}, d_{yz} < d_{x^2-y^2}, d_{xy}$.
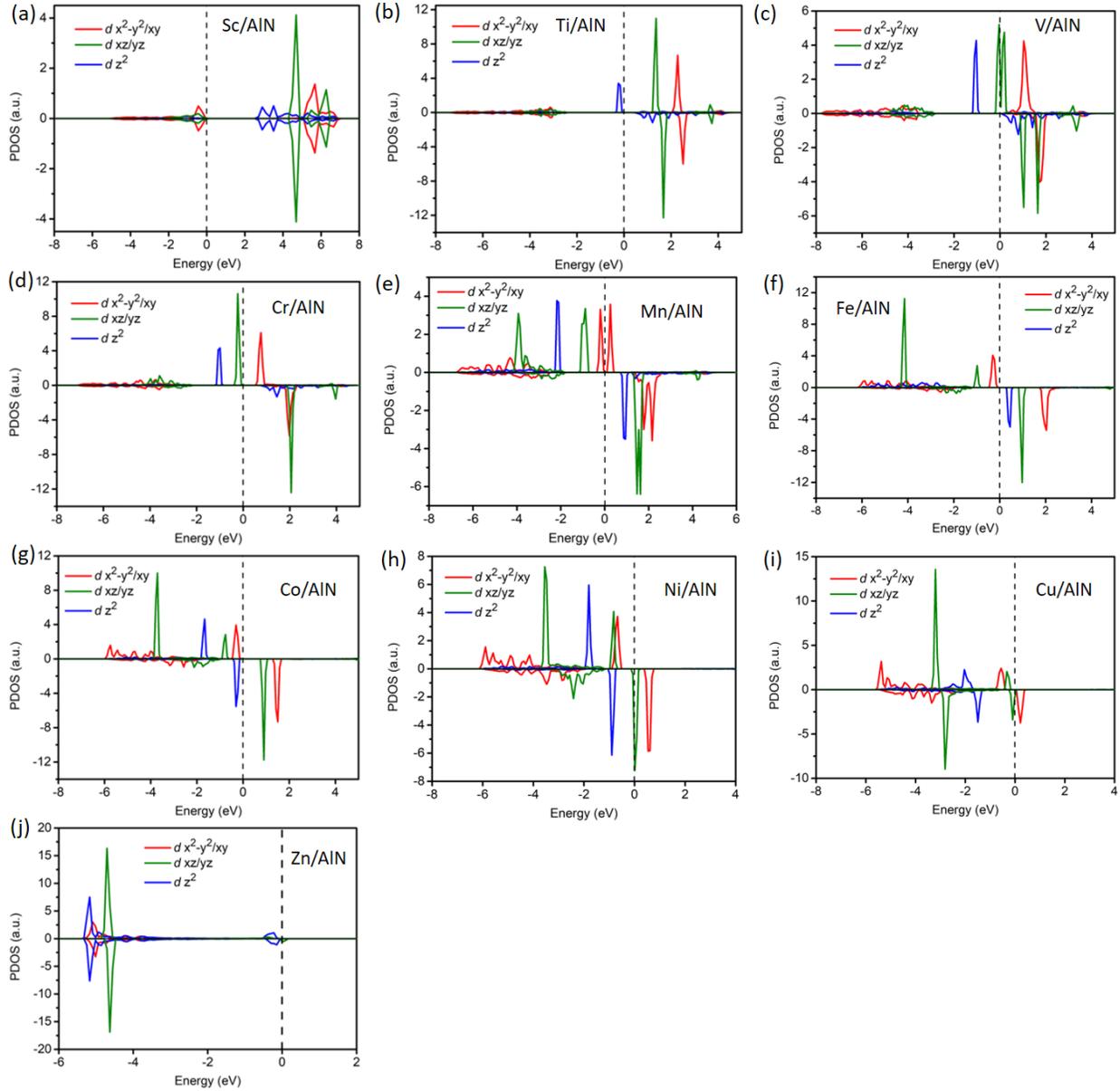
Figure S4. PDOS of the individual d orbitals of the TM-dopant atoms (a) Sc, (b) Ti, (c) V, (d) Cr, (e) Mn, (f) Fe, (g) Co, (h) Ni, (i) Cu and (j) Zn in AlN.
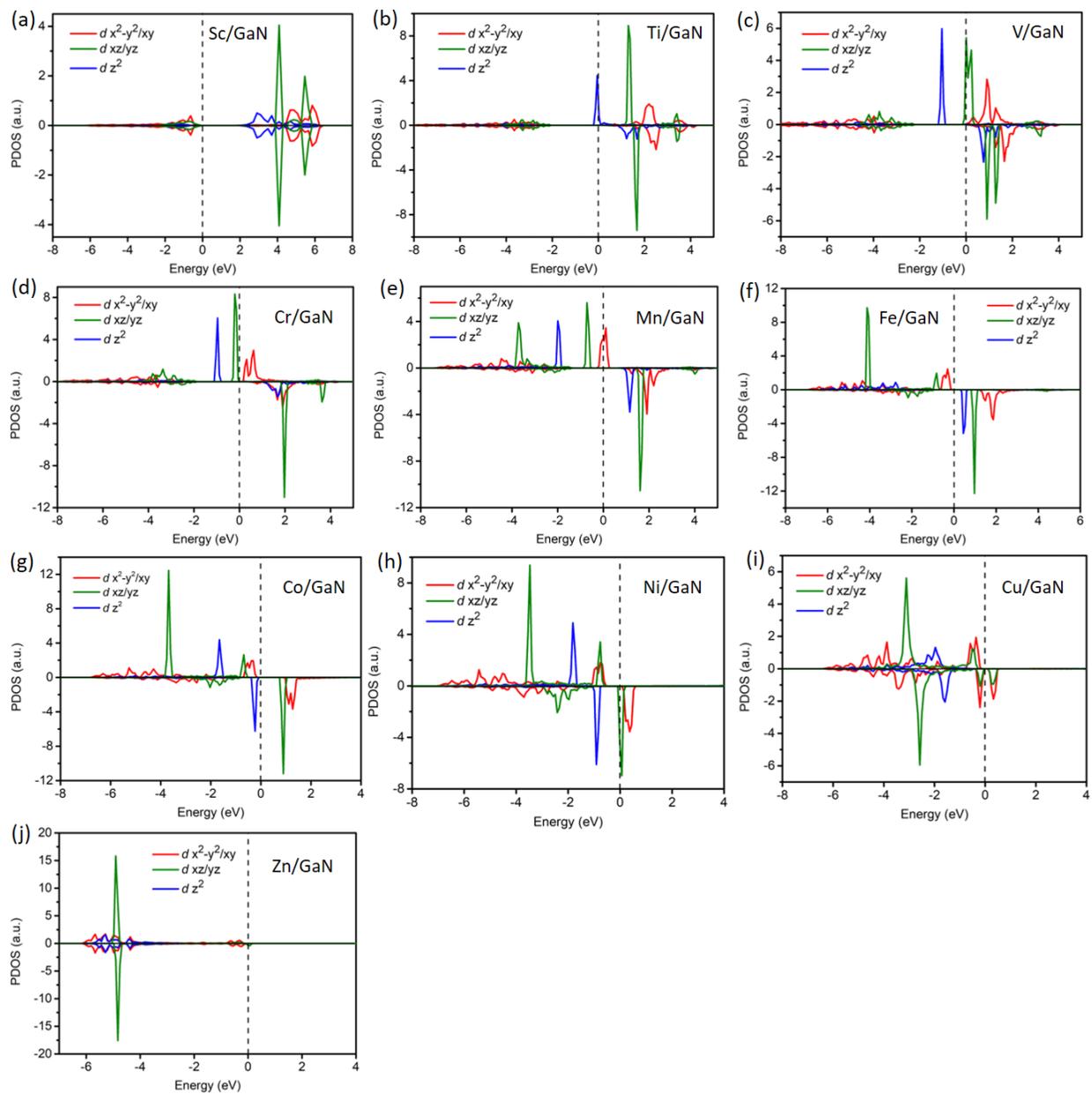
Figure S5. PDOS of the individual *d* orbitals of the TM-dopant atoms (a) Sc, (b) Ti, (c) V, (d) Cr, (e) Mn, (f) Fe, (g) Co, (h) Ni, (i) Cu and (j) Zn in GaN.

Spin-polarized PDOS of TM-doped AlN and GaN with adsorbed OH, O and OOH

Figures S6, S7 and S8 show the PDOS of TM ions, resolved into contributions of the individual d orbitals, with the OH, O, or OOH species adsorbed. After adsorption of one of these species, the TM ion is in a trigonal pyramidal symmetry environment, see Figure S1. This absorption does not change the degeneracies, but the energy ordering of the d states on the TM ions becomes $d_{xz}, d_{yz} < d_{x^2-y^2}, d_{xy} < d_{z^2}$.
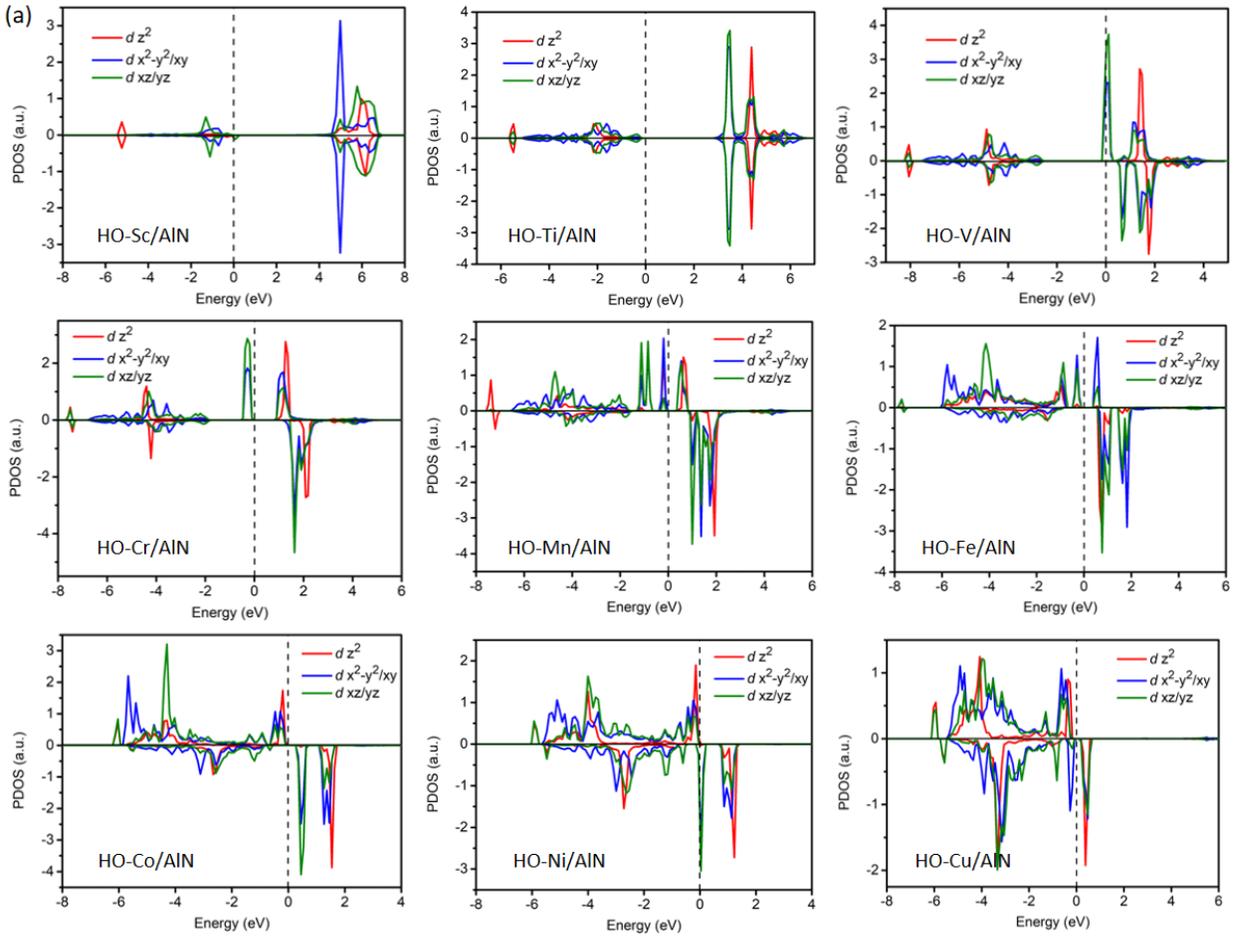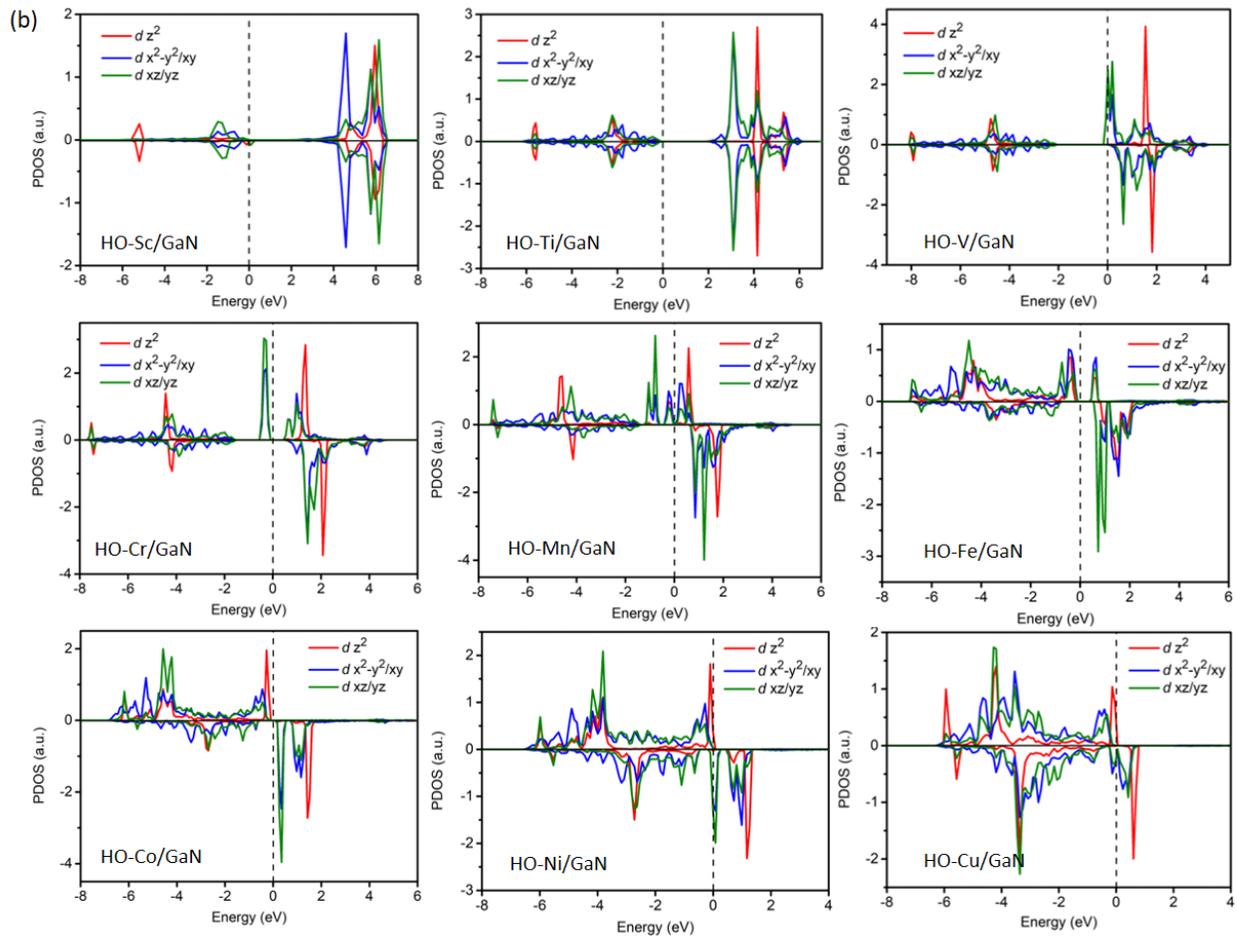
Figure S6. PDOS of TM-dopant atoms in (a) AlN and (b) GaN monolayers, with adsorbed OH.

(a)

16
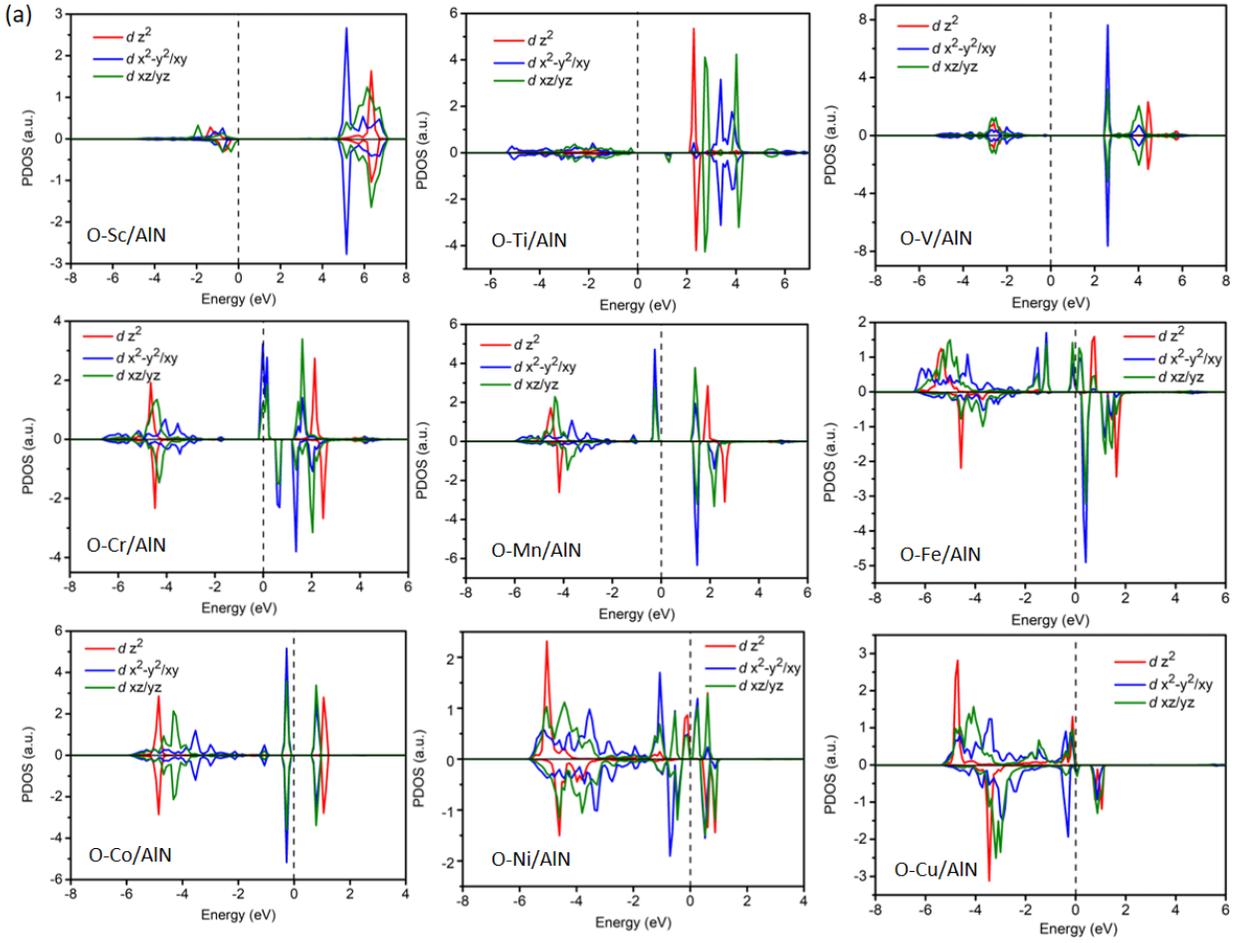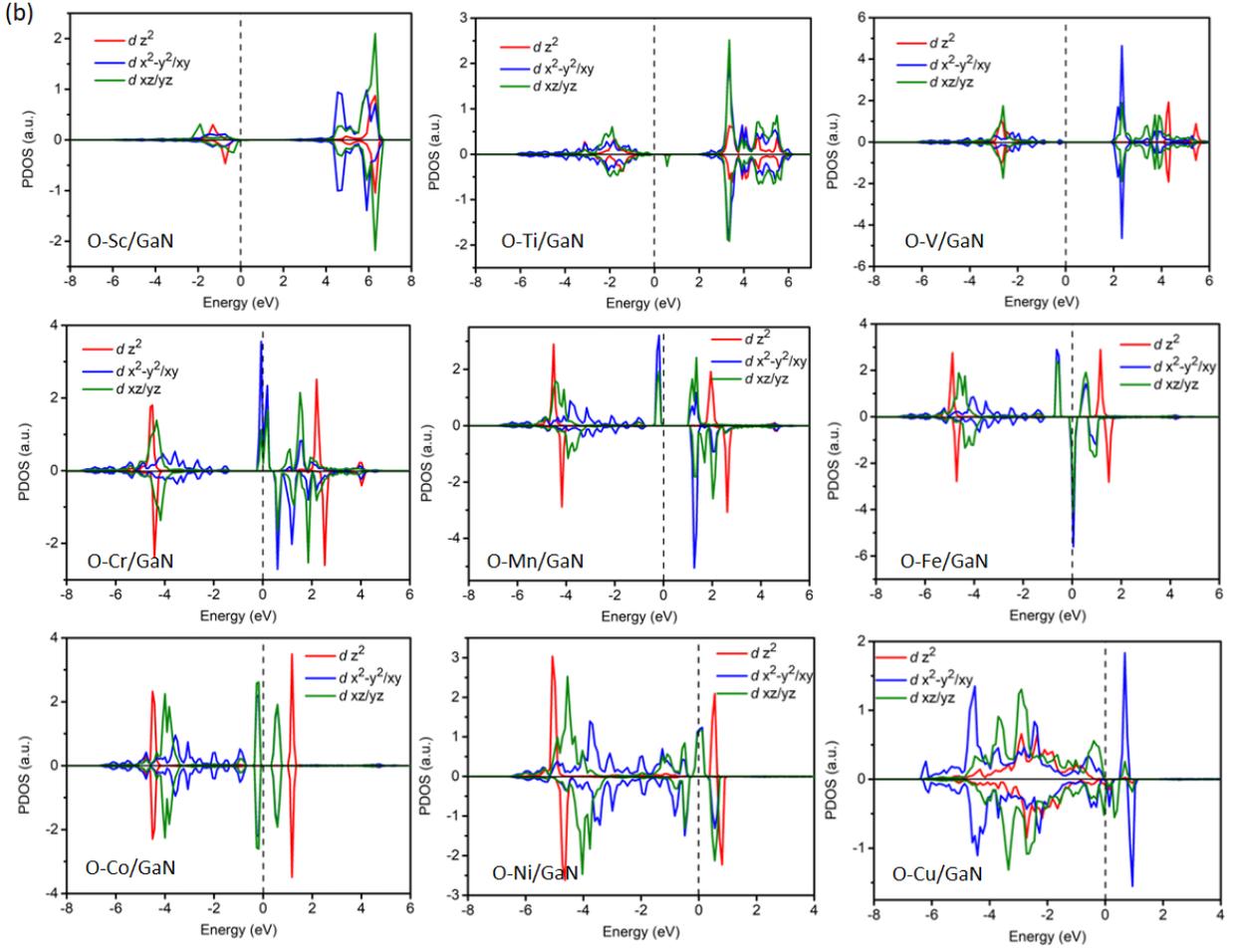
Figure S7. PDOS of TM-dopant atoms in (a) AlN and (b) GaN monolayers, with adsorbed O.
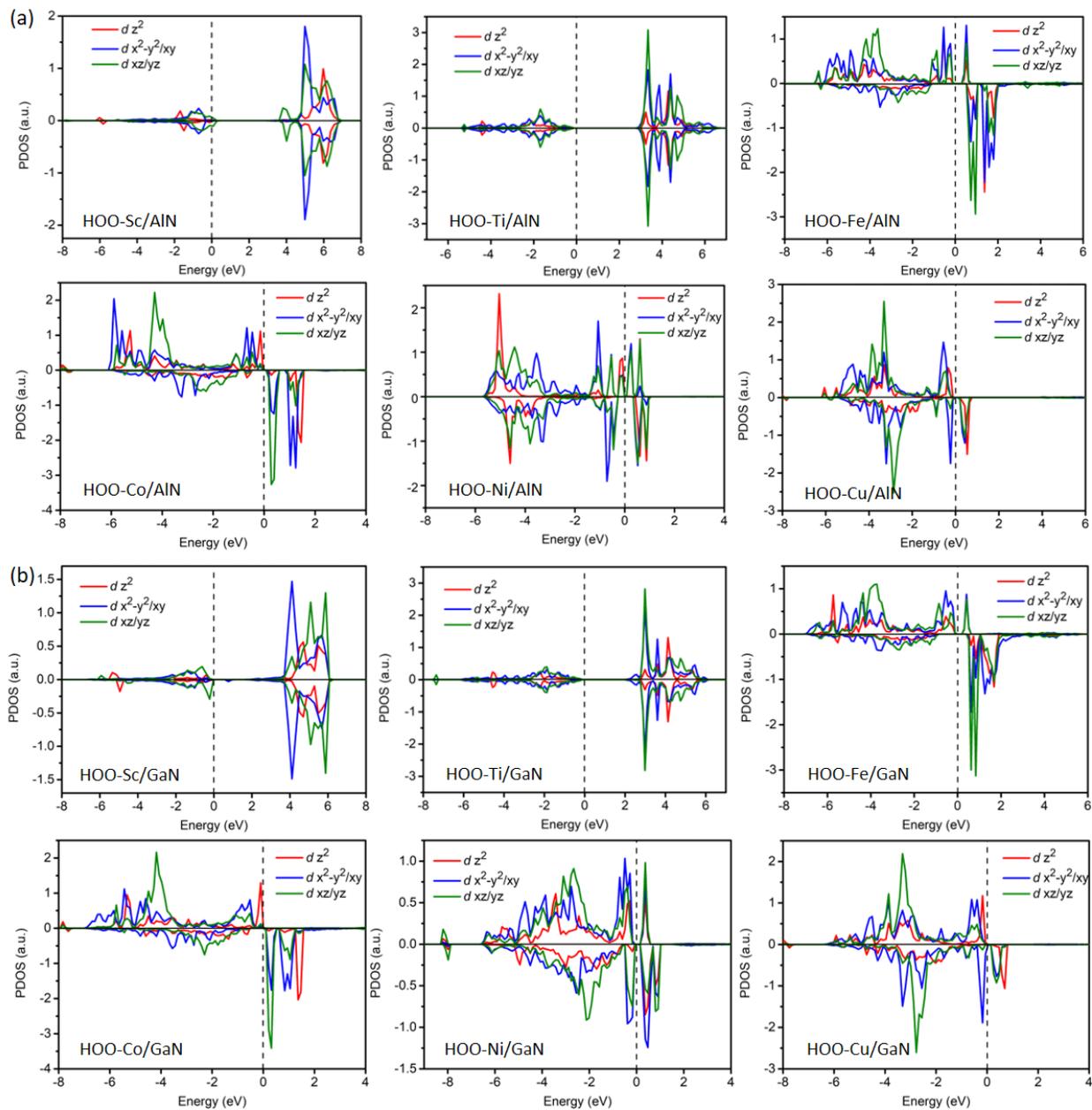
Figure S8. PDOS of TM-dopant atoms in (a) AlN and (b) GaN monolayers, with adsorbed OOH.

Magnetic moments of TM-dopant ions in AlN

Table S3 shows the magnetic moments on the TM-dopant ions in AlN. The exact values of course depend upon the specific procedure used by VASP to calculate the projections on the individual atoms. Nevertheless, comparison of the relative values, and to the values of the total magnetic moments given in Table 1 in the main text, should give an indication of how the magnetic moments are distributed. The magnetic moment on the TM-dopant ions in GaN are within a few percent of those in AlN. "/" means that the species does not adsorb stably or metastably.

Table S3. Calculated magnetic moments of the TM-dopant ions (in μ_B per supercell) in AlN.

System	Sc	Ti	V	Cr	Mn	Fe	Co	Ni	Cu	Zn
Nothing adsorbed	0.00	0.71	1.69	2.64	3.36	3.72	2.66	1.64	0.76	0.02
OH adsorbed	−0.02	0.00	0.93	1.84	2.63	2.99	2.92	1.86	0.89	/
O adsorbed	−0.08	−0.02	0.00	0.94	1.74	2.22	0.00	0.48	0.88	/
OOH adsorbed	−0.02	0.00	/	/	/	3.00	2.86	0.97	0.83	/

High-spin versus low-spin states

As discussed in the main text, for the O-Co/XN and O-Ni/XN systems (X = Al, Ga), the low-spin state is found to be more stable than the high-spin state, which is unlike adsorption on other TM dopants, where the high-spin state is most stable. Table S4 shows the calculated total magnetic moments and total energies of the high and the low-spin states of both systems, as well as the total energy difference, ΔE(*O), between high-spin and low-spin states. We did not find a stable structure for adsorption of the O species on Ni/AlN in the high-spin state, so that entry in the table is marked as "/".

Table S4. Calculated total magnetic moments (in μ_B per supercell), total energies, E(*O), (eV) for the high-spin and low-spin states of O-Co/AlN and O-Co/GaN, and the total energy difference, ΔE(*O), between high-spin and low-spin states. Positive ΔE(*O) means that the energy of the high-spin state is higher than that of the low-spin state. "/" means that the adsorbed O structure is unstable.

Systems	magnetic moment (high-spin)	E(*O) (high-spin)	magnetic moment (low-spin)	E(*O) (low-spin)	ΔE(*O)
O-Co/AlN	4	–227.11	0	–227.70	0.59
O-Co/GaN	4	–189.18	0	–189.70	0.52
O-Ni/AlN	5	/	1	–224.59	/
O-Ni/GaN	5	–186.02	1	–186.64	0.62

GGA+U calculations for Co/XN and Ni/XN

The Gibbs free energies in the main text are calculated using a standard GGA/PBE density functional. As the doped XN systems involve fairly localized d states on the TM dopant atoms, it is appropriate to look at GGA+U calculations, in particular if there is a competition between high-spin and low-spin states regarding which of the two is lowest in energy. Including an explicit on-site electron-electron repulsion U for each TM d orbital promote high-spin configurations, whereas standard GGA functionals have a tendency to over-promote low-spin situations. For most TM dopants, we find that, even with the GGA/PBE functional, the lowest energy configurations are high-spin, so a GGA+U calculation gives no qualitative difference. Exceptions are the O-Co/XN, O-Ni/XN, and HOO-Ni/XN, which are found to be low-spin with GGA/PBE, so we recalculate these systems with GGA+U.

Choosing a value $U = 3.8$ eV (Ref. 2), the calculated magnetic moments of the TM ions and the total magnetic moments per supercell are listed in Table S5, and the Gibbs free energies for each reaction step are listed in Table S6 (compare to Table S2). For the Co-dopant systems, the magnetic moment is zero for O-Co/XN without U (Table 1 in the main text), indicating a low-spin state, whereas the GGA+U calculation gives a high-spin state, signaled by a magnetic moment of 4 μ_B (Table S5). The overpotential also changes and goes down to a low value $\eta \approx 0.5$ V (Table S6). But, for the Ni-doped systems, the GGA+U calculation shows no change in the spin state, i.e., the lowest energy structures of O-Ni/XN and HOO-Ni/XN still have low spin, and those of Ni/XN and HO-Ni/XN still have high spin. The GGA+U calculation increases the overpotential by a mere 0.1-0.2 V, up to ~0.5 V, which is still a relatively low value (Table S6). Therefore, we conclude that the GGA+U calculations do not change the conclusions expressed in the main text.

Table S5. Magnetic moments (MM) of the TM ions and the total magnetic moments (TMM) per supercell (in μ_B) calculated with GGA+U, with $U = 3.8$ eV.[2]

Systems	MM of Co	MM of Ni	TMM Co	TMM Ni
Nothing adsorbed	2.91	1.80	4	3
OH adsorbed	3.12	1.90	5	4
O adsorbed	2.56	0.58	4	1
OOH adsorbed	3.07	1.16	5	2

Table S6. Gibbs free energies (eV) calculated for the elementary reaction steps, see Table S2, and the overpotential, calculated with GGA+U, with $U = 3.8$ eV.[2]

	Co_AlN	Co_GaN	Ni_AlN	Ni_GaN
ΔG_1	1.69	1.69	1.79	1.65
ΔG_2	1.75	1.68	1.49	1.61
ΔG_3	1.37	1.44	1.30	1.38
ΔG_4	0.11	0.11	0.34	0.28
η (V)	0.52	0.46	0.56	0.42

References

1. Nørskov, J. K.; Rossmeisl, J.; Logadottir, A.; Lindqvist, L.; Kitchin, J. R.; Bligaard, T.; Jonsson, H. Origin of the overpotential for oxygen reduction at a fuel-cell cathode. J. Phys. Chem. B **2004**, 108, 17886-17892.

2. Liao, P.; Keith, JA.; Carter, EA.; Water oxidation on pure and doped hematite (0001) surfaces: Prediction of Co and Ni as effective dopants for electrocatalysis. J. Am. Chem. Soc. **2012**, 1;134(32):13296-309.